Nonlinear dielectric metalenses: imaging and higher-order correlations

Christian Schlickriede[1], Sergey Kruk[2], Lei Wang[2], Basudeb Sain[1], Yuri Kivshar[2], and Thomas Zentgraf[1]
[1]*Paderborn University, Warburger Straße 100, D-33098 Paderborn, Germany*
[2]*Nonlinear Physics Centre, Australian National University, Canberra, ACT 2601, Australia*
E-mail: thomas.zentgraf@uni-paderborn.de

Abstract: We demonstrate the first highly efficient all-dielectric nonlinear metalens that realizes third-harmonic imaging accompanied by spatial third-order correlations carrying information about coherence effects. We describe this metalens analytically with a generalized nonlinear lens equation.

OCIS codes: 160.4330, 230.4320, 190.4400.

The advancement in all-dielectric metasurfaces led to the development of highly-efficient metalenses of sub-micrometer thickness. The concept has been transferred to the field of nonlinear optical metasurfaces, and recently both nonlinear focusing [1] and second-harmonic imaging [2] have been demonstrated. Importantly, it has been revealed that the wavefront control by nonlinear metasurface lenses is not governed by the conventional lens equations routinely used in linear optics to describe the image location and size. Therefore, modified nonlinear lens equations were suggested phenomenologically [2]. Here we design and study the first nonlinear dielectric metalenses based on the third-harmonic generation. We study experimentally and theoretically the nonlinear wavefront propagation of the generated light and the resulting image formation by using all-dielectric metalenses. We demonstrate focusing and nonlinear imaging of objects. For the first time to our knowledge, we demonstrate higher-order correlations of light with nonlinear metalenses – a functionality that is not available in linear optics.

The metalenses are created by nanopillar arrays made of amorphous silicon. Each nanopillar acts as a nonlinear nano-resonator generating a third-harmonic signal with a well-defined nonlinear phase. Hence, the third-harmonic wavefront control can be achieved via the nonlinear Huygens' principle [3]: we employ a number of different geometries of the nanopillars whereas all providing similar efficiencies of the third-harmonic generation (THG) combined with high forward directionality while adding different resonant phase delays from 0 to 2π to the THG process. In such a way, we realize an efficient wavefront control of the third-harmonic signal. The nanopillars are 600 nm high, and they are fabricated on a glass substrate by using standard electron beam lithography followed by a plasma etching process. Figure 1a shows an image of the fabricated metasurface. We fabricate a lens with a size of 200×200 µm and a focal distance of 400 µm. Figure 1b shows the experimental ray-tracing of a pump beam before ($z<0$) the metalens and the third-harmonic signal after ($z>0$) the metalens. Figures 1c and 1d show a clear focus spot formation of the third harmonic signal at the distance of 400 µm.

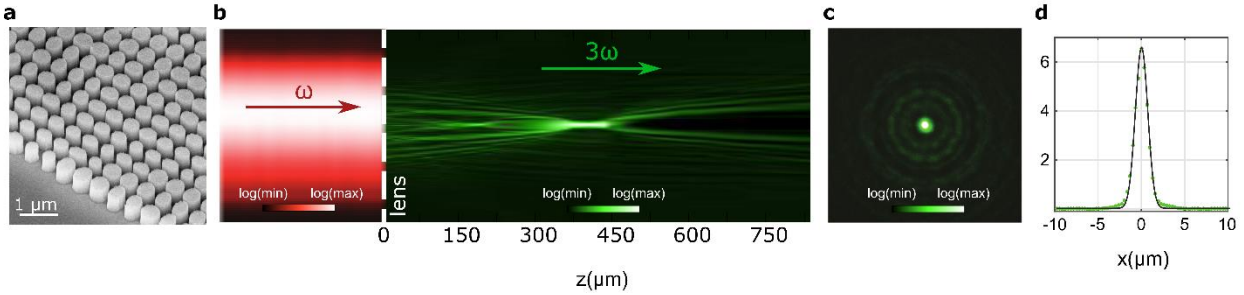

Figure 1 | Nonlinear all-dielectric metalens for the third-harmonic generation. a SEM image of a fabricated dielectric metalens. **b** Experimental distribution of the pump (red, left part) and third-harmonic (green, right part) intensities along the optical axis. Pump wavelength: 1550 nm, lens focal distance: 400 µm. **c** THG distribution at the focal plane (a logarithmic scale). **d** Cross-section of the THG distribution at the focal plane.

Next, we study experimentally the imaging performance of this nonlinear metalens with real objects while simultaneously converting the light to the third-harmonic field. For that, we image an L-shaped aperture (see Fig. 2a) placed in front of the lens. We observe a THG image that fits the phenomenological nonlinear lens equation proposed earlier in Ref. [2] and generalized here to the case of the third-harmonic generation,

$$1/f = 1/na + 1/b \ , \tag{1}$$

where a is an object distance, b is a distance to an image, and n is the nonlinear harmonic order (THG: n = 3). The THG image appears aberrated as the superposition principle of waves is not applicable to the nonlinear lens.

We further image a pair of circular apertures (see Fig. 2b). The THG image results in four circles (spots), which can be understood as follows: The larger outer circles are formed by 3ω-photons generated by ω-photons all coming from the same aperture (either top or bottom). The inner smaller circles are formed by three ω-photons generated by ω-photons from both apertures (e.g. one ω-photon from the bottom aperture and two ω-photons from the top aperture). Hence, the image formation is also associated with a third-order autocorrelation function of the apertures, not only showing the THG images of the object but also carrying an information about its coherence. By adding a third circular aperture (see Fig. 2c), we observe a similar correlation process, which shows two additional maxima between each of the two larger outer circles and additionally, one central maximum at 3ω resulting from ω-photons coming from each of the three circular apertures. Figure 2d graphically presents a simplistic explanation of origin of the autocorrelation effects. In order to characterize both the imaging and the autocorrelation, we comparatively perform analytical and numerical studies of the nonlinear wavefront that is generated at the metalens and propagates to the image plane and beyond. Additionally, for the 2-aperture experiment, we perform a THG ray-tracing along the optical axis in the vicinity of the imaging plane (see Fig. 2e).

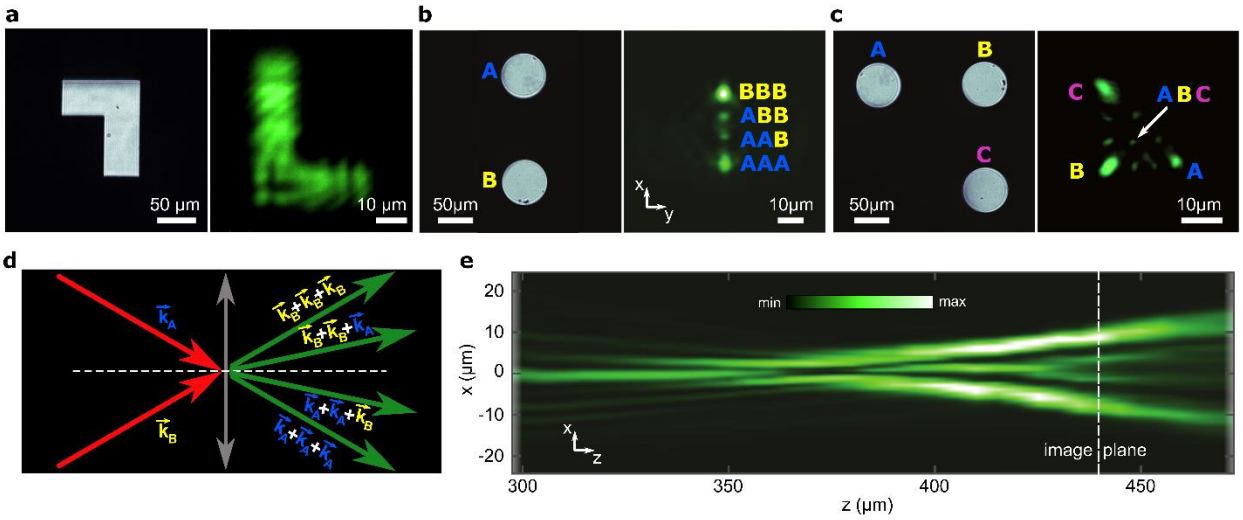

Figure 2 | Third-harmonic imaging with a nonlinear metalens and the observation of higher-order correlations. a Left: L-shape aperture placed in front of the lens and illuminated with a pump beam at 1550 nm wavelength. Right: its THG image after the nonlinear lens. **b** Left: Two circular apertures before the lens. Right: corresponding field distribution after the lens showing the formation of four maxima associated with the third-order autocorrelation function of the object. **c**. Three circular apertures (left) and corresponding THG formation of 10 maxima associated with the third-order autocorrelations. **d**. Conceptual illustration of the autocorrelation process in the THG lens. **e**. Experimental field distribution of the THG field along the optical axis near the imaging plane of the two apertures.

The third-order correlation effects accompany the third-harmonic imaging, and such lenses might have prospective advantages for applications in nonlinear optical information processing as well as spatial photon correlation and coherence measurements from objects.

Acknowledgements. We acknowledge a support from the Australia-Germany Joint Research Co-operation Scheme and the German Academic Exchange Service (DAAD).

References

[1] E. Almeida, O. Bitton, and Y. Prior, "Nonlinear metamaterials for holography", Nature Communications **7**, 12533 (2016).
[2] C. Schlickriede, N. Waterman, B. Reineke, P. Georgi, G. Li, S. Zhang, and T. Zentgraf, "Imaging through nonlinear metalens using second-harmonic generation" , Advanced Materials **30**, 1703843 (2018).
[3] L. Wang, S. S Kruk, K. L. Koshelev, I. I. Kravchenko, B. Luther-Davies, and Y. S. Kivshar, "Nonlinear wavefront control with all-dielectric metasurfaces", Nano Letters **18**, 3978–3984 (2018).